

Effects of Geocell Confinement on Strength and Deformation Behavior of Gravel

Ben Leshchinsky¹ and Hoe Ling, M.ASCE²

Abstract: In past years, railroad transportation has been of growing interest because of its efficiency and advancement in railway technologies. However, many issues arise because of the variability in subsurface conditions along the sizeable lengths of track that exist. One very important issue is the need for significant upkeep and maintenance for railways passing over areas of poor soil conditions as a result of continuous deformation and a lack of stiffness from the foundation. One general solution for lack of substructure integrity has been confinement, applied through a variety of reinforcement types, including geocell. To investigate the effectiveness of geocell confinement on substructure integrity, a series of embankment model tests with different configurations of geocell placement (one layer and two layers of geocell) were constructed and loaded monotonically and cyclically for comparison with unreinforced, control tests. On the completion of these tests, the model embankments were simulated numerically using finite-element procedures. The results, which matched reasonably well, were then used as validation for a parametric study, observing the effects of less competent geocell material, gravel, and foundation conditions and their implications. The tests and numerical simulations demonstrate that geocell confinement effectively increased stiffness and strength of a gravel embankment while reducing vertical settlement and lateral spreading. Additionally, the parametric study shows that the use of geocell provides a composite mattressing effect that distributes subgrade stress more uniformly than without reinforcement, increasing bearing capacity and reducing settlement, especially on soft foundations. The results suggested that in some site conditions, use of geocell might be an economical alternative to frequent maintenance and/or lower train speeds. DOI: [10.1061/\(ASCE\)GT.1943-5606.0000757](https://doi.org/10.1061/(ASCE)GT.1943-5606.0000757). © 2013 American Society of Civil Engineers.

CE Database subject headings: Gravel; Railroad tracks; Confinement; Deformation; Laboratory tests; Finite element method; Parameters.

Author keywords: Gravel; Railway; Confinement; Geocell; Reinforcement; Deformation; Laboratory tests; Finite element; Parametric study.

Introduction

Geocell has long been used as a means for improving soil conditions. It was originally developed by the U.S. Army Corps of Engineers to increase vehicular mobility over loose, sandy subgrade through cellular confinement (Webster and Alford 1977). Geocell has been shown to increase soil strength by confinement, reducing lateral spreading and causing the confined composite to behave as a more rigid mattress (Zhou and Wen 2008). The higher stiffness of the geocell system reduces the stress applied to the subgrade from bending stiffness of the mattress composite, similar to a slab (Pokharel et al. 2011). Several studies have shown that utilization of the cellular confinement mechanism significantly improves the strength and stiffness of a granular material; however, a lack of generic design methodology has inhibited its implementation (Han et al. 2008).

One particular application that could benefit from cellular confinement is ballasted foundations of railways. Ballast functions as a base that absorbs energy, drains easily, and resists forces acting vertically and laterally, providing a stiff competent foundation for the repeated loading exerted by train passes (Selig and Waters 1994). However, these important roles face significant technical issues that challenge the function of a working railroad. The pressures resulting from train loading can result in rearrangement and degradation of ballast over many loading cycles, reducing grain interlocking and facilitating lateral movement of particles (Lackenby et al. 2007). Track stability can decrease with the lateral spreading of ballast particles caused by decreasing frictional strength (Selig and Waters 1994). Vertical and lateral deformations as a result of spreading or foundation problems result in loss of track geometry. Retention of substructure geometry is vital to track function; the cost of track maintenance because of geotechnical issues is significant compared with other track expenses (Indraratna et al. 1998).

Ballasted railway foundations are supposed to be thick enough to ensure uniform loading of the subgrade at an acceptable intensity (Indraratna et al. 2006). The confinement mechanism from various geosynthetics, including geocell, has been shown to increase the strength and stiffness of the infill, which in turn distributes the stress to a larger area, especially on soft subgrades (Chrismer 1997; Zhou and Wen 2008; Yang 2010). It is possible that geocell-ballast composite action could enhance this mechanism, which is especially advantageous under the high loading intensity of moving trains. In addition to the redistribution of vertical stresses (Chrismer 1997), the confining behavior provided by reinforcements has been shown to

¹Assistant Professor, Dept. of Forest Engineering, Resources and Management, Oregon State Univ., 280 Peavy Hall, Corvallis, OR 97331; formerly, Ph.D. Candidate, Dept. of Civil Engineering and Engineering Mechanics, Columbia Univ., New York, NY 10027 (corresponding author). E-mail: ben.leschchinsky@oregonstate.edu

²Professor of Civil Engineering, Dept. of Civil Engineering and Engineering Mechanics, Columbia Univ., New York, NY 10027.

Note. This manuscript was submitted on September 12, 2011; approved on April 24, 2012; published online on April 26, 2012. Discussion period open until July 1, 2013; separate discussions must be submitted for individual papers. This paper is part of the *Journal of Geotechnical and Geoenvironmental Engineering*, Vol. 139, No. 2, February 1, 2013. ©ASCE, ISSN 1090-0241/2013/2-340-352/\$25.00.

reduce and/or redistribute shear stresses at the subgrade interface (Giroud and Han 2004). Because ballast is generally a highly frictional material, whereas the subgrade is often inferior, the reduction of shear stresses is highly beneficial. Some studies have suggested that use of geosynthetics, but especially three-dimensional (3D), cellular reinforcements like geocell, can improve ballast performance and stability, including a reduction in deformation (Raymond 2001), sustained track geometry (Chrismer 1997), and an increase in strength and resilience under cyclic loading (Indraratna et al. 2006). The increase in the confinement in the ballast from geosynthetics would reduce the strains encountered in the foundation as well (Indraratna et al. 2010).

To realize how geocell placement in gravel foundations can affect dimensional stability and stiffness, a series of gravel embankment model tests using poorly graded gravel was performed. Economic, time, and space constraints prevented direct, full-scale modeling of a ballasted embankment with true, American Railway Engineering and Maintenance-of-Way Association standard ballast gradations, but the slightly smaller material used in testing was still poorly graded gravel and considered demonstrative of similar behavior. A control test without geocell and two different geocell configurations, centrally placed layer of geocell and two layers of geocell confinement, were conducted. These embankments were loaded under two different conditions: monotonic and cyclic loading. The tests were then analyzed using commercially available finite-element (FE) analysis software for model validation and further application.

Laboratory Tests

Material Characterization

The mechanical properties of the poorly graded gravel (granite) were characterized by a series of four large-scale triaxial tests run under different confining pressures (61–95 kPa). Additionally, four cyclically loaded, large-scale triaxial tests were performed to study the behavior under repeated loading. The triaxial specimens were 30.5 cm in diameter and 61 cm tall and were confined using a 1-cm-thick soft latex membrane and a vacuum pump to apply confining pressure (suction) to the gravel. The gradation was attained from a sieve analysis (Fig. 1, GP, $D_{50} = 15.5$, $C_u = 1.67$, $C_c = 0.986$; Leshchinsky 2011) with mesh sizes of 4.75, 0.422, 0.152, and 0.075 mm (No. 4, No. 40, No. 100, and No. 200, respectively), using nonstandard larger sieves that were built to handle the large sample and grain sizes. The stiffness

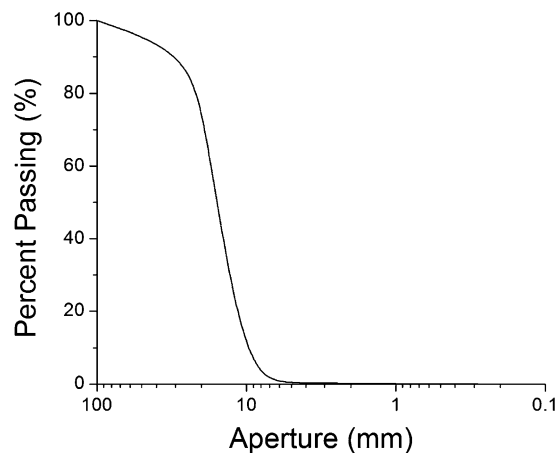


Fig. 1. Grain size distribution for model test

was obtained from the initial, linear portion of the loading curve attained from the triaxial tests (axial strain rate was 0.5%/min). Although the size of the particles used in laboratory testing was smaller because of expense constraints, it was still classified as poorly graded gravel, implying that it generally had the same mechanical behavior as larger, cohesionless, gravels used in ballast. Larger ballast particles could still effectively fit in the geocell used in experimentation. The angle of friction and angle of dilation were determined from the results of the triaxial tests (Fig. 2) and were found to be 45 and 15°, respectively. The in situ tested unit weight of the gravel was determined to be approximately 15 kN/m³.

Model Tests

The model embankment of height 55 cm and slope of 45° was set up on a RC floor that was 1 m thick (also called a strongfloor specifically for simulated testing; Fig. 3). The model was confined by a 10-cm-tall square wooden frame (152 × 152 cm) to serve as a consistent footprint for consecutive setup of tests in addition to preventing lateral movement along the smooth-surfaced concrete. Use of a concrete floor was a laboratory constraint; however, numerical validation of the tests would allow for further simulations on varying subgrades and different geometries. The model was prepared by first infilling the wooden frame with gravel and then placing five layers of approximately 9 cm on the base with no mechanical compaction (poorly graded granular material attains higher relative densities with little more than proper placement) and material being dispensed from an approximate drop height of 30 cm above grade. The structure does not simulate an actual railway foundation but instead is a truncated square pyramid made up of poorly graded gravel. Despite this difference, the model behavior studied during this

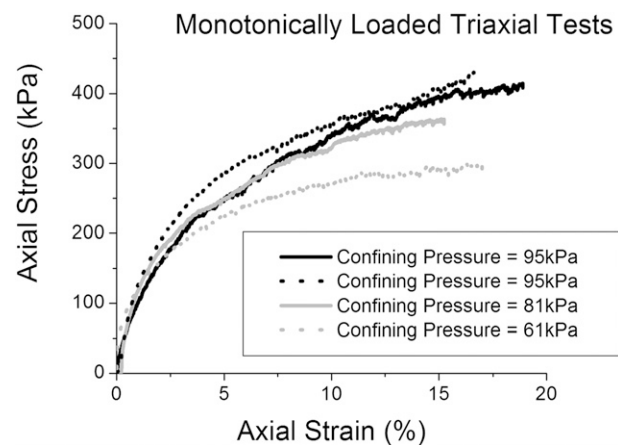


Fig. 2. Stress-strain results of monotonically loaded triaxial tests

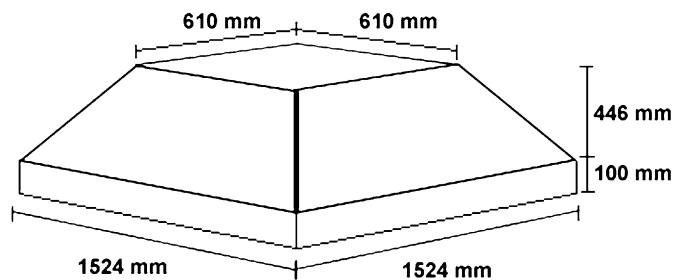


Fig. 3. Geometry of model

laboratory test is instructive on the relevant mechanical effects of geocell confinement (Leshchinsky 2011). Additionally, it served as a 3D verification of FE analysis leading to more complex studies on true embankment geometry.

The geocell was placed in two different configurations: centrally located in the embankment, and two layers in the embankment. As is suggested for installation, the geocell was outstretched when inflated. The geocell (height = 15 cm, sinusoidal diamond shape with length and width of 22.5×22.5 cm) was made from novel polymeric alloy (NPA), which was found to have a tensile strength of 27 MPa and a Young's modulus of 2.07 GPa. This polymeric alloy generally has a higher stiffness and strength than the common high-density polyethylene (HDPE) geocell, as well as a lower thermal expansion coefficient and creep reduction factor (Pokharel et al. 2011). Material properties were attained from a series of laboratory tensile tests, both monotonically and cyclically loaded (Fig. 4). These tests were run using an Instron tensile device with a strain rate of 2%/min and the specimen cut in a dog-bone shape to induce yield in a controlled fashion, tested at 23°C [corresponding to ASTM D638 (ASTM 2010)]. Strain was monitored by a series of strain gauges placed midheight on the interior of the cell walls, attached using an epoxy and then dried to ensure connection during testing.

The control tests were characterized by having no geocell confinement within the embankment. This serves as a basic comparison for other tests where geocell was added for reinforcement. The single reinforcement configuration consisted of a centrally placed layer of geocell confinement within the model, approximately 20 cm from the floor level (Fig. 5). The double reinforcement configuration was constructed of two layers of reinforcement: one approximately 10 cm from the floor and the other about 30 cm from the floor level (Fig. 5). All of these configurations were loaded under both monotonic and cyclic conditions on separate occasions to demonstrate the behavior of the embankment in both unconfined and confined conditions.

The load was applied to the embankment using an MTS loading actuator (manufactured by MTS Systems) that has 450-kN capacity. However, the reaction frame that held it in place was limited to only 80 kN. To ensure frame stability, it was secured into the 1-m-thick concrete strongfloor (Fig. 6). The load was applied to the embankment using a square steel loading plate with dimensions of 356×356 mm and 25 mm of thickness. The square shape of the loading plate was chosen because of the square shape of the prism's crest and a need for load symmetry.

Under monotonic loading, the embankment was loaded with a constant displacement rate of 2.54 mm/min until failure. The actuator was paused at approximately every 6.35 mm of vertical displacement to allow for some manual data collection. This necessary action is the cause of the spiked shape in the loading curves. However, the shape of the curves suggests that this pause had a negligible effect on the overall model behavior and results.

The cyclic tests consisted of 50,000 cycles of loading at a frequency of 5 Hz, with sinusoidal loading cycles representative of vibrations that might occur from wheel loads either caused by the setup of the axles and bogies or load transmission from nearby passing freight. Additionally, it was chosen with the interest of applying the maximum possible number of loading cycles allowable within the time and equipment restrictions enforced by the laboratory. During this test, lateral displacements were recorded at 0, 1,000, 5,000, 10,000, 20,000, 30,000, 40,000, and 50,000 loading cycles. The test was stopped at 50,000 cycles for logistical reasons (time/resources).

The loading amplitude for the unreinforced test was between 35 and 175 kPa, which was 20% of the maximum load attained from the monotonic test. This minimum was chosen to ensure accurate loading frequencies as lag may occur when the lowest amplitude is too small. Additionally, the stress under the tie is often higher than zero during train passes, even when the wheel load is not on top of it. The loading amplitude for both of the reinforced configurations was between 70 and 350 kPa, representative of realistic load.

During the loading stages, the behavior of the embankment was monitored, including lateral displacement, vertical displacement, vertical load, and strain in the geocell. The vertical displacement was measured by the actuator. The lateral displacement was recorded at three different heights, measured from the concrete floor, 30, 45, and 55 cm (crest), to capture the spreading along the cross section of the embankment. The lateral displacement was determined by measuring the movement of light, near-frictionless sliding arms that were in contact with wooden plates on all four sides of the model slope (for redundancy), whose accuracy was confirmed using a laser displacement transducer. After each test was completed, a gradation analysis was performed (to observe gravel integrity), the geocell was exhumed (to determine damage when applicable), and the data were analyzed to determine a vertical yield stress and apparent stiffness of the embankment.

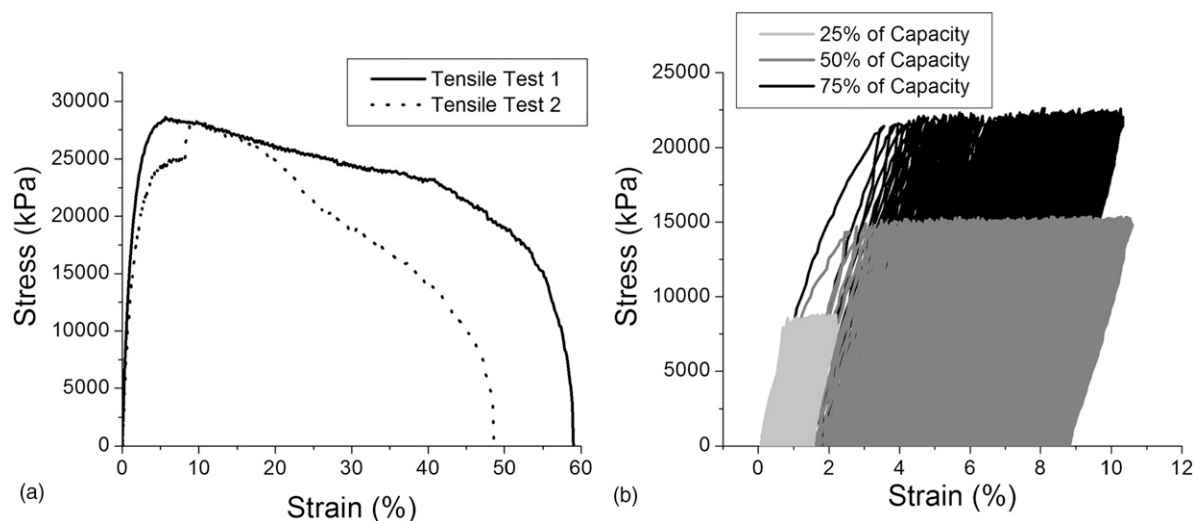


Fig. 4. Stress-strain results of (a) monotonically and (b) cyclically loaded geocell tension tests

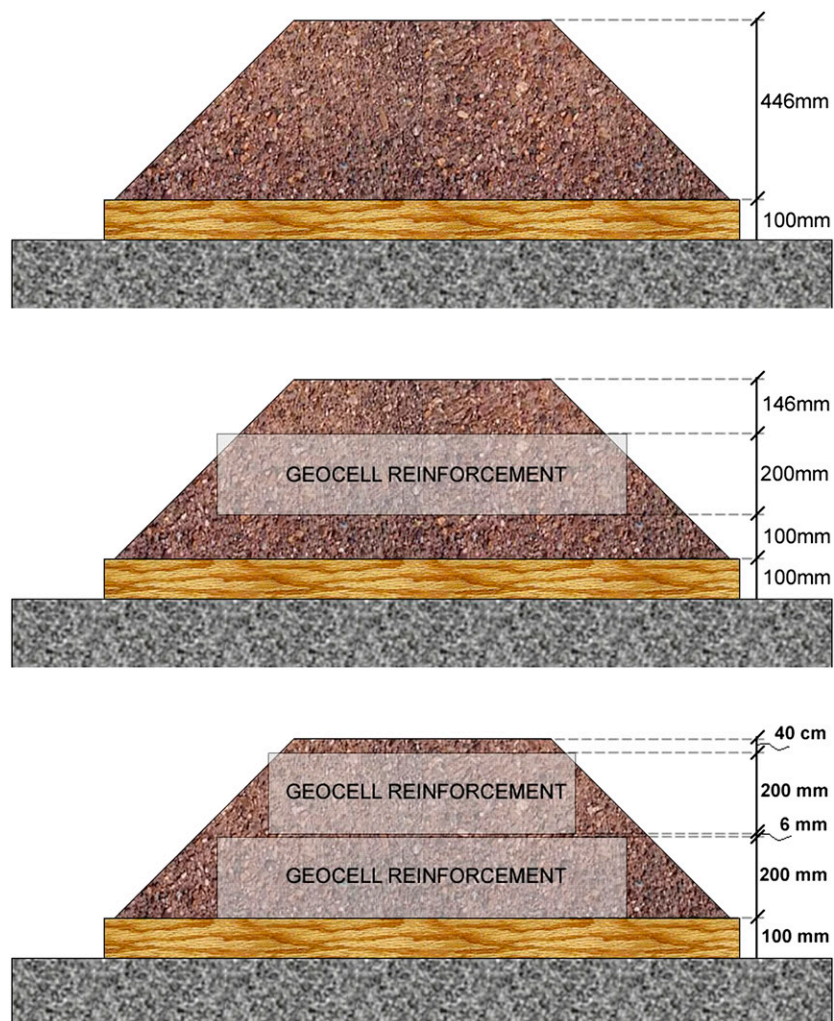


Fig. 5. Cross-section of reinforcement configurations

Test Results

Monotonically Loaded Tests

The apparent vertical stiffness of the embankment, represented by the initial, linear portion of the load-displacement curve, was attained from the results of each monotonically loaded test (Table 1). In the case of no geocell (Test 1), the apparent stiffness was approximately 4.5 kPa/mm of vertical displacement. The model tests with one layer of geocell (Test 2) demonstrated an approximate stiffness of 10.9 kPa/mm, and the double layer (Test 3) had 11.9 kPa/mm. The results showed that the geocell confinement allowed significant stiffness gains of 2.4 and 2.6 times greater than the unreinforced case for Tests 2 and 3, respectively.

Additionally, the yielding or failure behavior of the embankment under monotonic loading was observed. In the unreinforced test, failure occurs at approximately 175 kPa in vertical stress, signified by the continuous vertical displacement occurring for the same load. Defining failure was not as simple in the reinforced tests because of the loading limit allowed by the frame and the significant increases in strength enabled by the geocell. The final loads were 575 and 625 kPa for the single- and double-reinforced tests, respectively. In the embankment confined by only one layer of geocell, there was a slight loss of linearity in the load-displacement relationship at the

higher loading levels, yet no defined yielding. The test was stopped because the applied load was close to the allowable tensile limit for the loading frame. On exhumation of the geocell, it was evident that some tearing at the seams directly underneath the loading plate occurred.

The double-reinforced embankment reached the tensile limit for the loading frame, yet no loss of linearity in the vertical load-displacement curve suggests no yielding had yet occurred and that more load could likely be sustained. Both layers of exhumed geocell were in good condition, showing no rupture and little bending. Strain gauges confirmed that very small strain was encountered during testing, where maximum lateral tensile strains of 0.5 and 2.1% occurred in the cell under the loading plate for the single- and double-layer tests, respectively (rupture coupled with strain-gauge issues in the single-layer case prevented full capture of strains). The geocell confinement allowed significant strength gains of at least 3.3 and 3.6 times larger than the unreinforced case for Tests 2 and 3, respectively (the failure load for both setups was likely higher). The use of two layers of geocell ensured better structural integrity in the reinforcement, especially under higher loads.

Vertical displacement under monotonic loading was greatly reduced with geocell confinement. At 175 kPa of vertical loading, the vertical displacement that occurred was 65, 23, and 21 mm for the unreinforced, single-reinforced, and double-reinforced configurations, respectively (Fig. 7). In the unreinforced embankment,

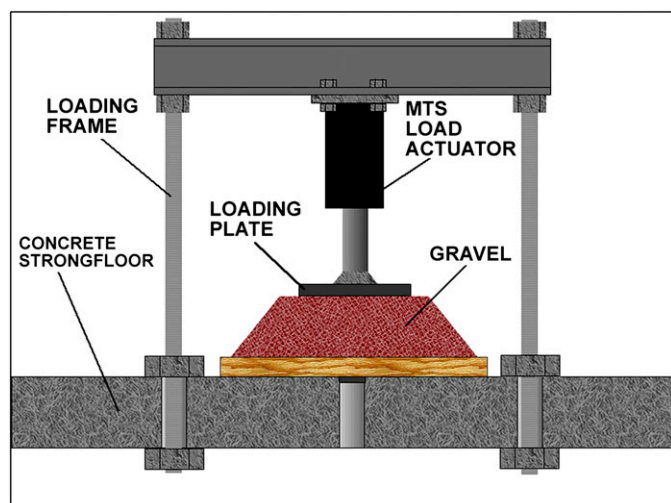


Fig. 6. Schematic of testing apparatus

Table 1. Summary of Results from Monotonically Loaded Model Tests

Measurement	Test 1	Test 2	Test 3
Reinforcement layout	Unreinforced	Single layer	Double layer
Maximum stress (kPa)/load (kN)	175/22 (Failed)	575/72.7 (Stopped)	625/79.1 (Stopped)
Yield vertical displacement (mm)	65	60	53
Apparent stiffness (kPa/mm)	4.5	10.9	11.9

significant lateral displacements occurred throughout the lateral cross section of the model, especially at the crest. The lateral displacement measured along the slope in the unreinforced test was 108 mm (31% increase in width) at the crest, 30 mm (6.6% increase in width) at the middle (45 cm from floor), and 20 mm (3% increase in width) at the bottom (30 cm from floor). Lateral displacements under monotonic loading were reduced because of the confining mechanism of geocell. Compared with the unreinforced test, the use of one layer of geocell inhibited the lateral spreading greatly, reducing the displacement at the crest, middle, and bottom portions by 42, 41, and 51%, respectively. Use of two layers of geocell was even more effective, reducing the displacement at the crest, middle, and bottom portions by 79, 45, and 51%, respectively. Much of the spreading that occurred in both reinforced tests occurred at the crest, directly above the geocell confinement (Table 2). Gradation analyses ran after testing demonstrated negligible changes in the gradation, likely because of the quality of the material used.

Cyclically Loaded Tests

Use of geocell confinement reduced the amount vertical deformation that occurred in the embankment under repeated loading. At the end of the unreinforced test, the vertical displacement caused by cyclic loading was 118 mm, which was close to the maximum stroke distance of the actuator. However, the final vertical displacement for the single- and double-reinforced cases was 62 and 57 mm (52 and 48% of displacement that occurred in control test with double the stress amplitude), respectively (Table 3).

The unreinforced embankment did demonstrate minimal stiffening under repeated loading, yet there was still significant deformations

occurring at the finish of the 50,000 cycles. This continuous deformation of the embankment under repeated loads is likely because of the low confining pressures encountered in the unreinforced model, preventing further lateral movement of the gravel. However, both of the geocell-confined tests demonstrated significant resilient stiffening under repeated vertical loading as shown by the flattening of the curves in the displacement-log(cycle) plot (Fig. 7).

Large lateral displacements occurred in the unreinforced test, especially at the middle and crest portions on the model. The lateral displacement measured along the slope in the unreinforced test was 36.1 mm (10% increase in width) at the crest, 55.3 mm (12% increase in width) at the middle (45 cm from floor), and 23.4 mm (3.5% increase in width) at the bottom (30 cm from floor). Use of geocell greatly reduced the lateral deformations occurring at the middle and bottom areas of the slope. Compared with the unreinforced test, the use of one layer of geocell reduced the displacement at the middle and bottom portions by 76 and 70%, respectively, although the lateral displacement at the crest was similar to the unreinforced case (which could be because of higher loading amplitudes and the considerable depth, 14 cm, of unconfined material overlying the geocell). Use of two layers of geocell was more effective, reducing the displacement at the crest, middle, and bottom portions by 30, 18, and 21%, respectively (Table 4). Similar to the monotonic tests, much of the spreading that occurred in both reinforced tests occurred at the crest, directly above the geocell confinement.

The geocell in both configurations encountered only cosmetic damage from the cyclic loading. That is, only superficial scraping occurred on the cell walls and slight bending taking place at the top and bottom lip of the geocell (Fig. 8). On exhumation, there was no tearing at the seams or rupture, and insignificant bending at the top lip of the cells. Strain gauges confirmed that little cumulative strain or creep occurred during the 50,000 cycles of loading, with a maximum lateral tensile strains of 2.5 and 1% (top layer, midheight on interior of cell wall) under the loading plate for the single- and double-layer tests, respectively (less than 0.5% tensile strain for central cell in bottom layer of geocell). Similar to monotonic testing, gradation analyses ran after testing demonstrated negligible changes in the gradation.

Finite-Element Analysis

A commercially available FE software, *ABAQUS* (Hibbitt, Karlsson and Sorensen Inc. 2007), was used in the analysis. The six model tests were simulated using material properties attained from laboratory tests and the geometry and boundary conditions, and the stress and deformation behavior was compared. Similar to the laboratory tests, these simulations consisted of three static and three cyclic loading conditions. Validation through numerical modeling adds credibility of further analysis simulating more practical applications. A 3D analysis is necessary to accurately simulate the confining mechanism of geocell reinforcement when applied to poorly graded gravel foundations.

Material Properties

To correctly characterize the materials used in testing and attain reasonable results in the FE analysis, reliable material data must be used.

The gravel was modeled as a nonassociative elastic-plastic material, obeying 3D Drucker-Prager (D-P) yield criterion, which is commonly used to simulate granular materials because its strength and yield are dependent on volumetric strain (dilation) and stress level. The D-P model was chosen for simplicity in modeling the elastic-plastic behavior of the gravel using a rounded yield surface as

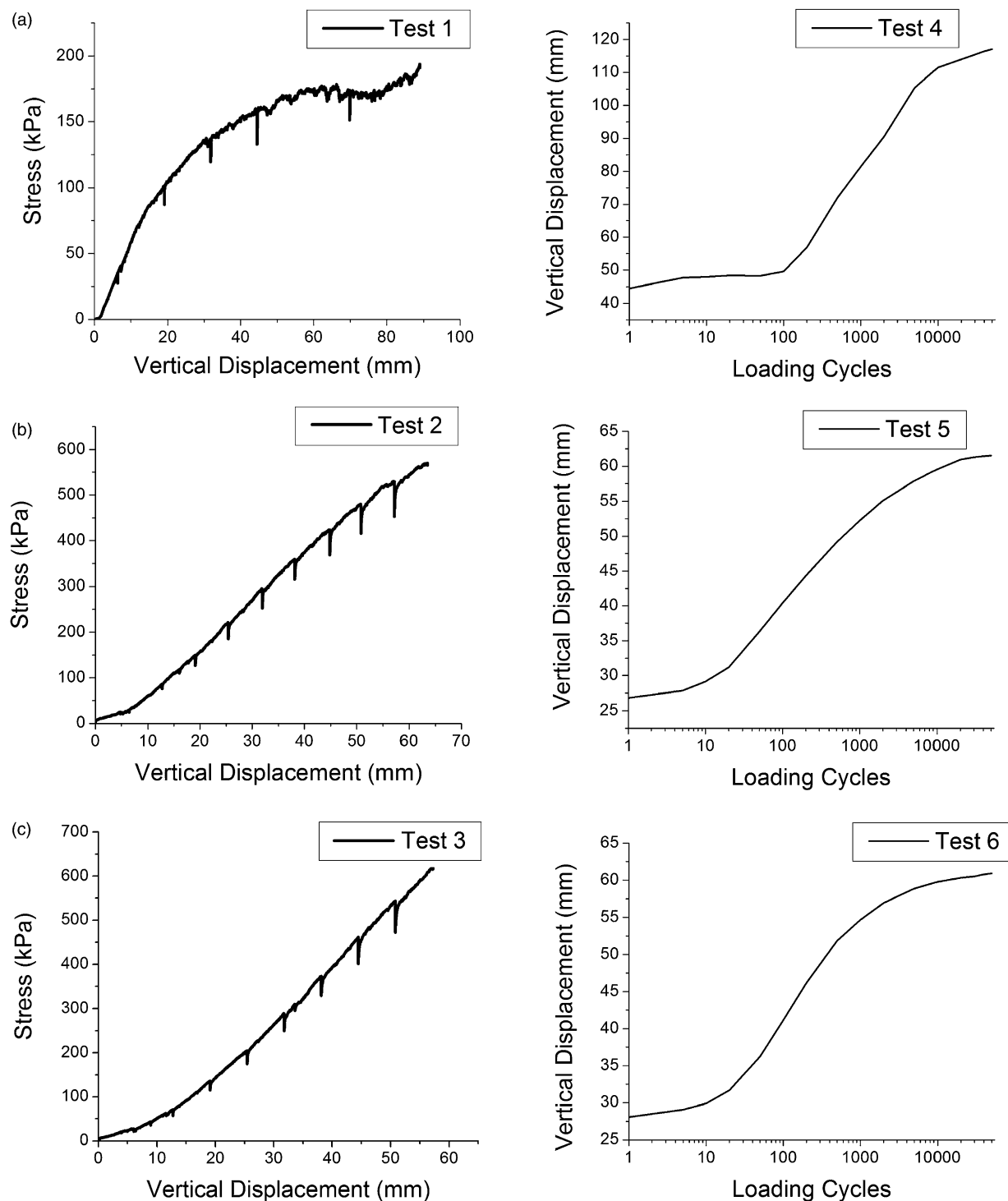


Fig. 7. Load-displacement curves for (a) Tests 1 and 4, no geocell confinement; (b) Tests 2 and 5, single layer of geocell; and (c) Tests 3 and 6, double layer of geocell

opposed to the sharp drastic yield surface that exists in the stress space when using Mohr-Coulomb failure criteria. Additionally, the material parameters for the D-P model can be determined in a straightforward manner. Material models exist that could capture the behavior of the gravel with slightly more accuracy, especially under cyclic conditions, but would require considerably more parameters (some difficult to attain), introducing potentially less accurate and misleading results. However, results deemed that the D-P constitutive model was adequate in simulating the final

settlement excluding the hysteretic behavior of the embankment. The stiffness and strength properties were attained from triaxial tests (Fig. 2). The poorly graded gravel, a cohesionless material, was given a small cohesion (1 kPa) to assist with convergence issues while not critically affecting the results (Table 5).

The geocell was modeled discretely as an elastic material because only minimal damage and plastic strain were encountered during the tests (Table 5). The contact between the cell walls and the gravel (and gravel-loading plate interface) was modeled as hard normal contact

Table 2. Summary of Lateral Displacement from Monotonically Loaded Model Tests

Measurement Location	Displacement (mm)			Increase in width (%) ^a		
	Test 1	Test 2	Test 3	Test 1	Test 2	Test 3
Top, 546 mm ^b	108.0	63.5	22.2	31.5	18.5	6.5
Upper middle, 457 mm ^b	30.0	12.2	13.6	6.6	3.0	3.4
Lower middle, 305 mm ^b	20.1	10.2	10.2	3	1.8	1.8

^aPercentage increase compared with initial width.^bHeight measured from concrete strongfloor.**Table 3.** Summary of Results from Cyclically Loaded Model Tests

Measurement	Test 4	Test 5	Test 6
Reinforcement layout	Unreinforced	Single layer	Double layer
Final vertical displacement (mm)	118	62	57
Cyclic vertical displacement (mm)	74	36	34

Table 4. Summary of Lateral Displacement from Cyclically Loaded Model Tests

Measurement Location	Displacement (mm)			Increase in width (%) ^a		
	Test 4	Test 5	Test 6	Test 4	Test 5	Test 6
Top, 546 mm ^b	36.1	36.5	25.4	10.5	10.7	7.4
Upper middle, 457 mm ^b	55.3	13.3	10.2	12.1	3.3	2.5
Lower middle, 305 mm ^b	23.4	7.0	4.9	3.5	1.3	0.9

^aPercentage increase compared with initial width.^bHeight measured from concrete strongfloor.

(cannot penetrate cell wall), and the tangential frictional coefficient was specified as tangent of two-thirds of the internal angle of friction [$\tan(2/3\phi) = 0.666$], as is commonly used for soil-reinforcement interaction and is within general agreement of large-scale interaction shear test values from similar tests (Ling et al. 2009). The shape of the geocell was modeled with a rhomboidal shape as opposed to the actual pseudosinusoidal shape that is used in the tests. This was done to simplify meshing while still maintaining the basic mechanical function of confinement. Other 3D FE models of multiple cells of geocell have modeled the cells in a diamond, rhomboidal shape (Yang 2010).

The loading plate was modeled as a rigid material because the stiffness of the steel is orders of magnitude larger than the gravel.

Boundary Conditions

A quarter of the embankment was modeled to simulate the deformations as accurately as possible, while only requiring reasonable computational time. To ensure that the geometrical symmetry can allow this computational advantage, boundary conditions must be modeled correctly. Several displacement restrictions were applied to the embankment. Both of the interior, side faces were restrained from moving laterally, but allowed to move vertically because they lie in the center of the symmetrical embankment, where no lateral deformation is expected (Fig. 9). Also, the base of the embankment was fixed from displacing vertically, modeling the rigid concrete foundation underlying the gravel in the model tests.

Elements/Mesh

The baseline tests (1 and 4) were meshed using a structured pattern made up of 9,500 hexahedral, eight-noded, reduced integration

**Fig. 8.** Cosmetic damage to geocell consisting of only minor bending and scraping**Table 5.** FE Properties of Ballast and Geocell

Material Property	Ballast	Geocell
Mass density, ρ (kg/m ³)	1,520	950
Elastic modulus, E (kPa)	2,000	2,070,000
Poisson's ratio, ν	0.35	0.35
Internal angle of friction, ϕ (degrees)	45	
Angle of dilation, ψ (degrees)	15	
Cohesion, c (kPa)	1	

elements (C3D8R). The general simplicity of the embankment shape in addition to the absence of a complex 3D reinforcement embedded within allowed for the use of a simple meshing pattern.

The single-reinforced tests (2 and 5) were meshed using a semi-structured pattern that consisted of 17,520 tetrahedral, four-noded, reduced integration elements (C3D4R), which modeled both the gravel and geocell. The irregular geometry that arises from the use of a 3D reinforcement with a complex structure requires tetrahedral elements because of the wide variety of angles and dimensions encountered. The shape of this element serves a competent alternative to the eight-noded brick element used in the unreinforced test but requires many more nodes and subsequently more computational time.

The double-reinforced tests (3 and 6) were also meshed using a semi-structured pattern that consisted of 14,630 tetrahedral, four-noded,

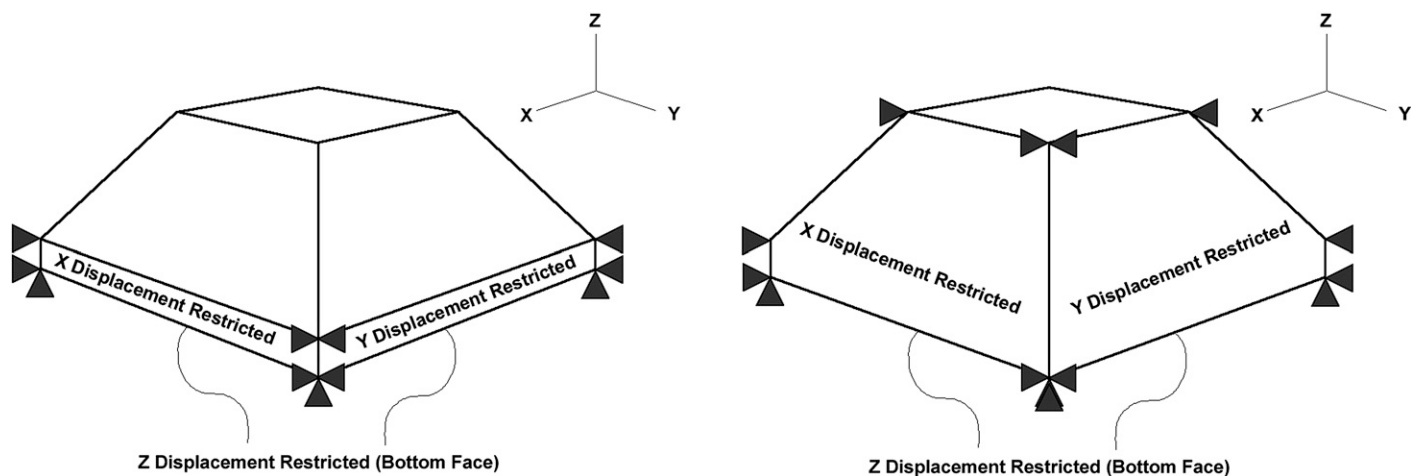


Fig. 9. Boundary conditions for quarter embankment geometry

reduced integration elements (C3D4R), which modeled both the gravel and geocell. Again, similar to the previous simulations with one layer of geocell, the irregular geometry that arises from the use of a 3D reinforcement with a complex structure requires tetrahedral elements because of the wide variety of angles and dimensions encountered.

Despite the lack of perfectly congruent meshes used for the three reinforcement configurations, all of the elements were generally meshed to a similar size (about 1.5 cm in diameter). This is an important consideration because meshing too finely might misrepresent the coarse gravel used in the actual test ($D_{50} \approx 1.5$ cm), whereas meshing too coarsely could have a similar detrimental effect.

Loading Stages

Static

Two loading stages were applied to the embankment quarter to simulate the loading conditions. First, gravity was applied to simulate construction and in situ conditions of the model test. It also allows the gravel to gain frictional strength as overburden pressure enables mobilization of its internal strength.

The next loading stage consisted of applying pressure to the crest of the model using a steel loading plate. *ABAQUS/Explicit* (Hibbitt, Karlsson and Sorensen Inc. 2007) was used to simulate the static loading applied to the embankment in displacement-control conditions while maintaining computational stability. In this stage, the displacement was slowly and steadily increased at a rate of 0.1 mm/s to those attained in the actual experiments. The vertical stress/displacement behavior was monitored throughout the simulation for comparison.

Cyclic

Two loading stages were applied to the embankment quarter to simulate the cyclic loading conditions. First, gravity was applied to simulate construction and in situ conditions of laboratory test, the same as modeled in the static case.

Next, dynamic conditions were simulated using *ABAQUS/Explicit* (Hibbitt, Karlsson and Sorensen Inc. 2007) to expedite the simulation by reducing computational time and to account for the inertial effects of the gravel. In this situation, a vertical pressure was applied to a loading plate placed on top of the crest, similar to static conditions. However, the load was applied cyclically, undergoing the same load amplitudes endured in the laboratory tests, along with

the same frequency. The simulations required approximately 30 h to run on a 32-GB RAM, 2.66-GHz server.

Monotonically Loaded Tests

The three statically loaded embankment tests were simulated using similar loading conditions and model geometry. Two geocell configurations were used: a single, centrally placed layer of geocell and two layers of geocell placed within the embankment. The actual experiment and the FE simulation were run in displacement-control conditions. Throughout the duration of these simulations, the vertical displacement and stress under the loading plate, as well as the lateral displacement along the profile of the embankment, were compared with the actual test results.

While comparing the vertical displacement to vertical load, it is shown that the results match reasonably well (Fig. 10). This is likely because of the use of quality laboratory data (triaxial tests of gravel, tensile tests of geocell) to characterize the material properties required by the FE analysis. These tests allowed an accurate determination of properties such as the internal friction angle, gravel stiffness, and geocell stiffness, which are necessary for analyzing this behavior.

However, the lateral displacements did not match entirely. This could be because of the difficulties in predicting the plastic deformation behavior in anisotropic cohesionless materials that are subject to low confinement pressures, such as much of the gravel at the crest or along the profile where much of the lateral spreading occurred. Despite the imperfect modeling of the lateral spreading occurring along the profile of the embankment, the general trends matched, and the displacement simulations were all within the same order of magnitude of the experimental results (Fig. 10).

The FE analysis is particularly useful in observing the stresses and strains in the geocell to examine possible weaknesses. As observed during the experiment and afterward, when the geocell was exhumed, the highest concentrations of stresses and strains occurred at the bottom corners of the diamond-shaped cells, under the loading plate. Intuitively, this makes sense because the bending of the gravel-geocell composite places significant tensile stresses on the lower part of the geocell, especially in the center region that happens to be some depth under the loading plate. This observation is important because, although the geocell underwent mainly elastic deformations during the testing, the polymer material can yield throughout the cell wall or the seam under higher loading. The stress concentration observed at the cell corners accentuates the need for

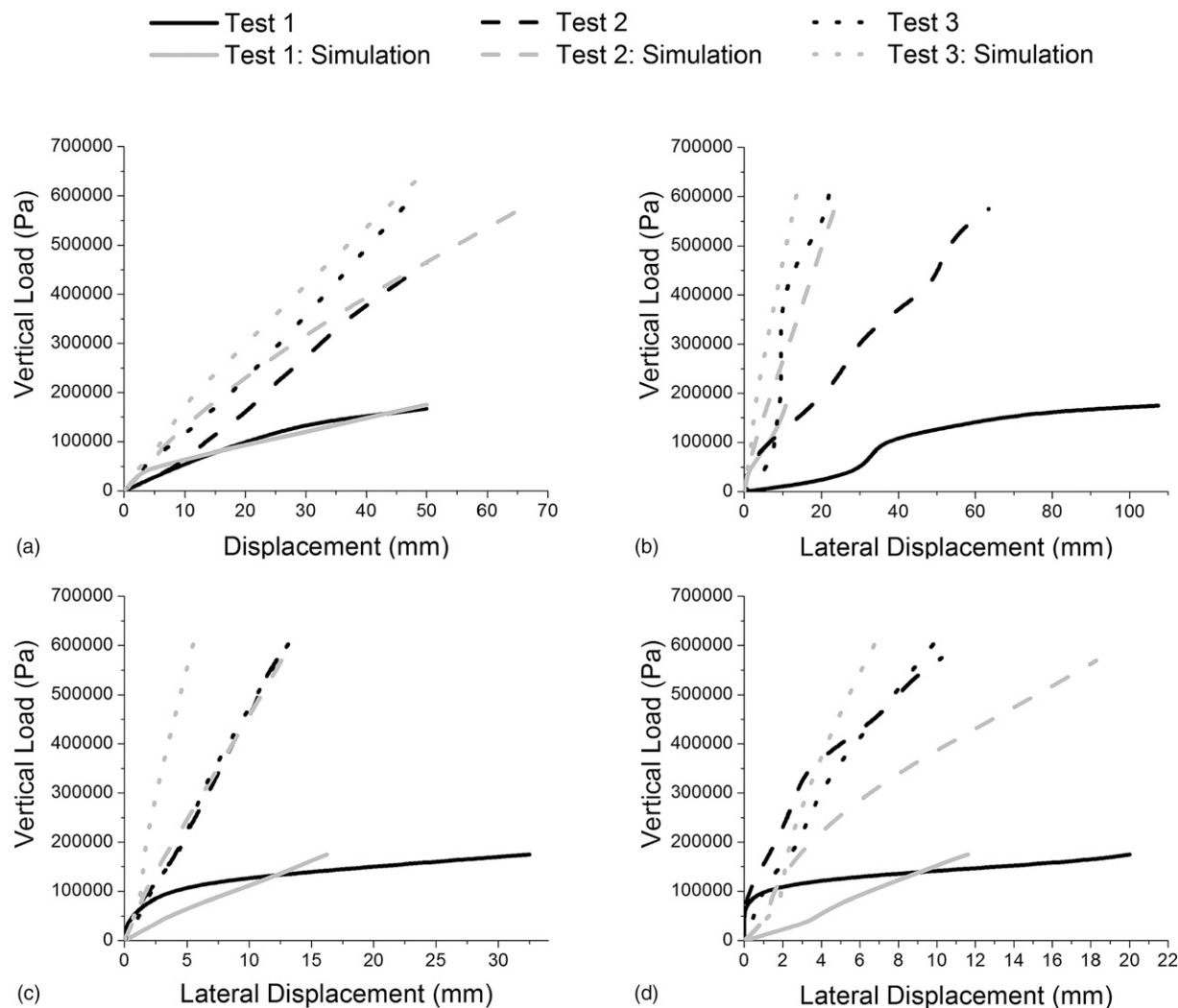


Fig. 10. Monotonic loading curves: (a) vertical settlement; lateral deformation at (b) crest, (c) middle, and (d) bottom

higher seam strength, which is often critically weak in comparison with the tensile strength of the walls forming the cells. Despite these concerns, strain gauges used in the geocell during experimentation implied that the geocell exhibited mostly elastic strain (i.e., recoverable strains), allowing the assumption of elastic behavior in the geocell for the FE analysis. The strains encountered in the critical regions of the geocell during the simulation were in the same range as those found in the experiments. In the single-layer reinforced test, the strains encountered in the geocell under the loading plate were 3.5 and 2.1% at bottom corner seam and central cell wall, respectively. Measured at the same geocell locations in the double-layer reinforced test, the strains encountered in the geocell under the loading plate in the top layer were 2.4 and 1.4% and in the bottom layer were 1.8 and 1.1%, respectively (Fig. 11).

Excluded from the analysis of the geocell was any simulation of creep, which can be a very complex and difficult process to simulate or predict. The material used for the geocell is an alloy that contains materials to inhibit creep behavior over time. However, the long-term creep might be a key concern, depending on material properties or a specific geocell application.

Although some of the simulated displacements did not match reality perfectly, the simulations and experiments were a good indicator to the advantages attained from using geocell confinement, including lower deformations and higher strength and stiffness.

Cyclic Tests

The three cyclically loaded embankment tests were simulated using similar loading conditions and model geometry. That is, the pressure was applied to the plate in load-control conditions, using a specified maximum and minimum load. An unreinforced control test and two reinforcement configurations were used: a single, centrally placed layer of geocell and two layers of geocell placed within the embankment. Throughout the duration of these simulations, the vertical displacement and stress under the loading plate, as well as the lateral displacement along the profile of the embankment, were compared with the actual test results.

Again, it was shown that the comparison of vertical displacement to vertical load matched reasonably well, at least for the unreinforced configuration (Fig. 12). However, the high stiffness of the geocell yielded relatively low estimates for vertical settlements encountered in either of the geocell model simulations. Generally, the cyclic hardening encountered by both of the reinforced models in the later loading stages was captured (as implied by the flattening of the curves in the later cycles), whereas the unreinforced configuration still underwent some cyclic deformation in both the experiment and the simulation. However, the magnitudes of the final vertical settlements simulated for both of the reinforced cyclic tests were not accurate. The fact that both Tests 5 and 6 encountered the same

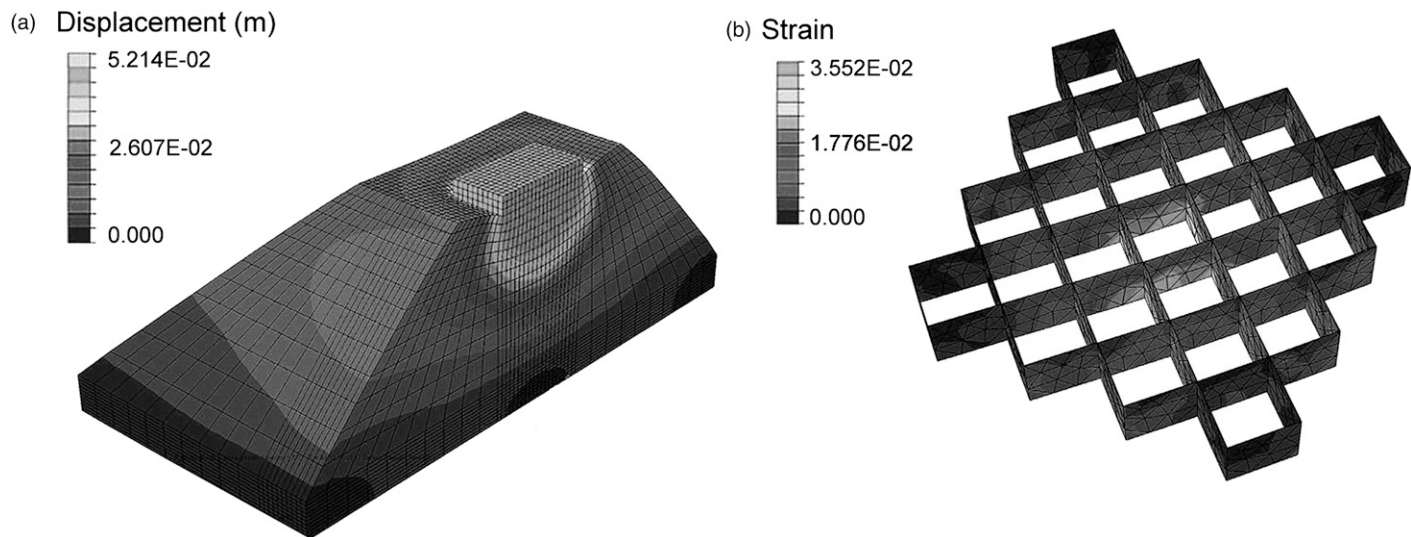


Fig. 11. (a) Test 1 displacement; (b) Test 2 strain in geocell

vertical displacement at the end of the test, a counterintuitive observation, was difficult to account for in the simulation. Despite this disagreement for the reinforced tests, the experimental results and simulations still demonstrate the benefits of using the geocell confinement in the gravel.

Regardless of some numerical discrepancies, the FE analysis did capture the advantageous trend that the single-reinforcement configuration did prevent further lateral spreading throughout the embankment profile, and the double-reinforcement configuration even more so. The actual simulated amounts of lateral displacement from the FE analysis did not match entirely, although they were reasonable (Fig. 12). Despite this, the simulation and experimental results indicate the significant reduction in deformation attained from using geocell confinement.

Strains observed in the geocell during experimentation were in the same range with those found in the FE analysis, both of which exhibited elastic behavior. Similar to the monotonic testing, the highest stresses and strains were found in the lower corners of the geocell that lied beneath the loading plate. In the single-layer reinforced test, the strains encountered in the geocell under the loading plate were 3.6 and 2.3% at bottom corner seam and central cell wall, respectively. Measured at the same geocell locations in the double-layer reinforced test, the strains encountered in the geocell under the loading plate in the top layer were 1.2 and 1.1% and in the bottom layer were 1.1 and 0.8%, respectively. Creep was not modeled. It would be difficult to observe creep under the limited amount of loading cycles applied and the time period of the experiment.

Parametric Study

A numerical parametric study was performed on the model geometry to observe its performance under varying geocell stiffness, gravel strength, and overlying over a soft foundation. Each time a parameter was varied, the model was in three configurations: an unreinforced control test, one layer of centrally placed geocell confinement, and two layers of geocell confinement. Insight into the resulting behavior demonstrates the benefits of using geocell confinement in gravel foundations. Under each condition, the vertical settlement under the loading plate and the maximum stress at the gravel-subgrade interface (to demonstrate the improvement in the stress distribution) was monitored when vertical load of the plate had reached 150 kPa. The settlement and subgrade stress behavior for each reinforced case

(under each changed parameter) was normalized to using the related, unreinforced case through the following relationships:

$$\frac{S}{S_u} = \text{Normalized Settlement}$$

$$\frac{q}{q_u} = \text{Normalized Maximum Stress}$$

S and q = vertical settlement under the loading plate and maximum stress at the gravel-subgrade interface, respectively. Similarly, S_u and q_u = vertical settlement and maximum stress at the gravel-subgrade interface for the unreinforced model embankment, respectively. The effects of geocell stiffness were demonstrated by placing the model over a 2-m-deep soft foundation (simulated by a stiffness of 1 MPa). Then, all three embankment setups were run using geocell stiffness of 0.1, 1, 2.07, and 200 GPa to demonstrate a variety of materials including HDPE, NPA, and structural steel. Use of HDPE, NPA, and steel in Tests 2 and 3 displayed significant added performance as the results show a significant reduction in settlement (75 and 82%, respectively) and maximum subgrade stress (35 and 40%, respectively) with the increasing geocell stiffness (Fig. 13). The effects of foundation stiffness were demonstrated by placing the model (reinforced with NPA geocell) over a 2-m-deep foundation with varying stiffness. The foundation stiffnesses of 1, 10, 100, and 100 MPa were used to demonstrate a range from soft to very stiff subgrades. The benefit of confinement was significant on a soft foundation as it decreased settlement and maximum stress at the subgrade significantly. As the foundation stiffness increased, the uniformity in stress distribution was lost (reductions of 3 and 20% for Tests 2 and 3, respectively), but settlement was still greatly reduced (87 and 90% for Tests 2 and 3, respectively) by preventing lateral spreading (Fig. 13). This is likely because the foundation stiffness was higher than that of the gravel, and the geocell-gravel composite action caused by confinement provides a more competent soil structure. Geocell reinforcement was beneficial on both soft and stiff foundations because it reduces settlement.

After many loading cycles, ballast deteriorates, becoming rounded, becoming contaminated by fines, and losing some of its strength (Indraratna and Salim 2002), eventually requiring replacement or maintenance. Thus, it was important to study the effects of gravel

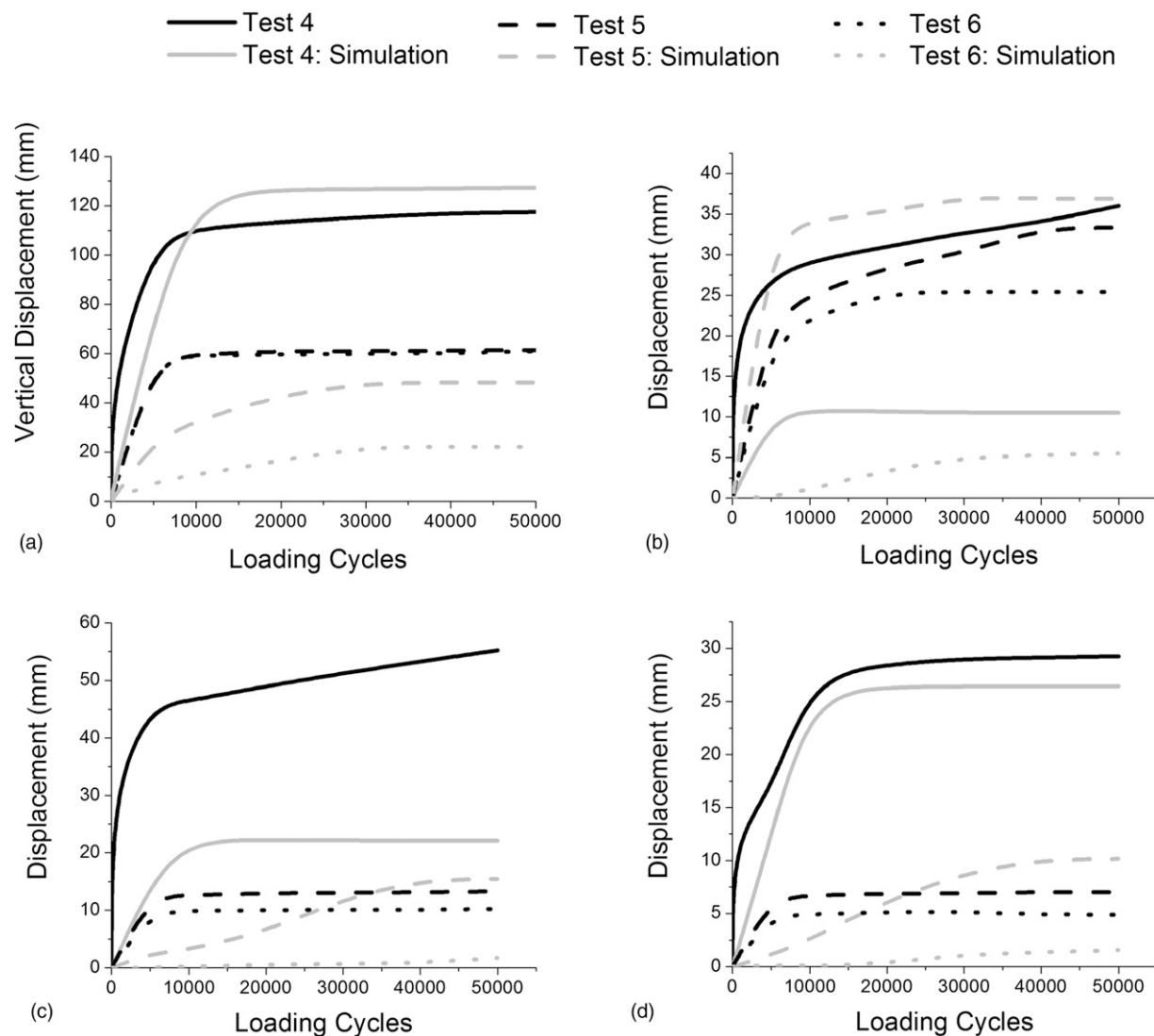


Fig. 12. Cyclic loading curves: (a) vertical settlement; lateral deformation at (b) crest, (c), middle, and (d) bottom

quality by altering the angle of internal friction (the governing strength parameter for a cohesionless material like gravel) between 25 and 55°, representing both very weak and very strong gravel. The embankment was placed above a 2-m-deep soft foundation (stiffness was 1 MPa).

The vertical settlement with a soft subgrade (1 MPa) is greatly reduced (between 60 and 75%) using a single layer of geocell and even more so with two layers. This benefit is attained for a range of frictional strengths in the gravel for the double-layer configuration and above approximately 33° for the single layer (Fig. 13). However, it did not vary greatly because the use of geocell confinement allowed the embankment to act as a composite, providing dimensional stability that is less dependent on gravel strength properties. Considering that all of these simulations occurred on a soft subgrade as opposed to a rigid subgrade, the benefit of geocell is shown by the great disparity between unreinforced and the reinforced cases.

The gravel friction angle had a significant effect on the subgrade stress distribution. At higher strengths, both geocell configurations provided a similar decrease in maximum subgrade stress (28 and 33% for Tests 2 and 3, respectively) in comparison with the unreinforced case. At lower strengths, there was little change in maximum stress at the subgrade interface (3 and 25% reduction for Tests 2 and 3, respectively). As expected, the double-reinforced case

yields a significant benefit here as it maintains a more uniform distribution even under very low strength because the entire embankment acts a composite. However, the plot suggests that it may not be an economical choice to use two layers of geocell as opposed to a single layer for reasonable gravel properties (40° and above), because the two reinforcement cases have similar benefits over the unreinforced case (Fig. 13). Despite this, both reinforcement configurations demonstrate a considerable gain in performance because of geocell confinement under several different conditions.

The strains in the geocell were in the recoverable, elastic range of values in the models discussed at a vertical load of 150 kPa. The compressibility of the foundation had a marginal effect on strain, yielding a range of maximum strain between 0.4 and 0.6% and 0.4 and 0.6% for the single- and double-reinforced configurations, respectively. Changing the stiffness of the geocell had a larger effect, as expected. Lowering the stiffness of the material allows much more strain for the same load. The range of strains varied between 4.5 and 0.02% and 3.2 and 0.01% for the single- and double-reinforced configurations, respectively. However, for HDPE and NPA, the maximum strain was about 0.6%, well within the elastic behavior for both materials. The strength of the gravel had an effect on the strain in the geocell, although it was not critical. Larger strains,

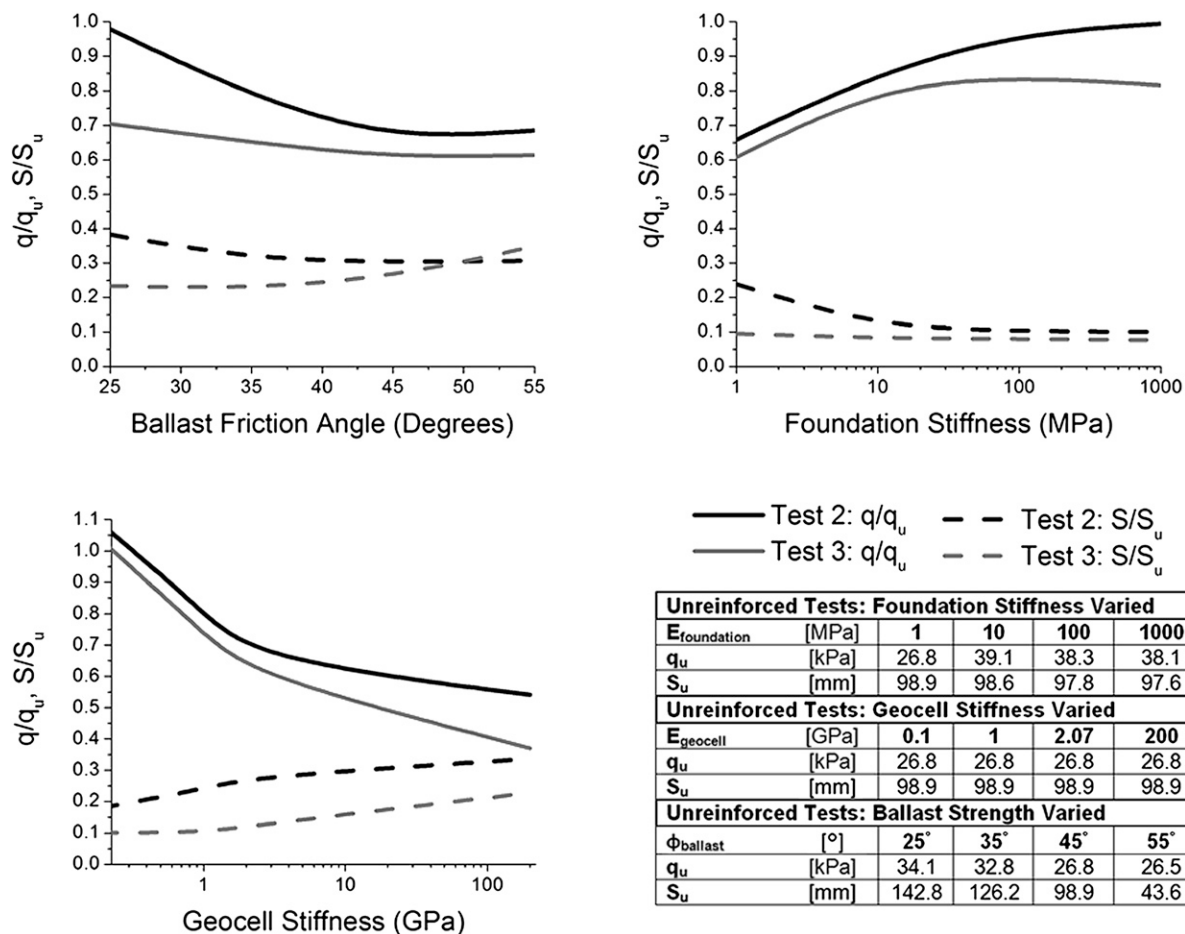


Fig. 13. Settlement and maximum subgrade stress normalized using results from unreinforced case

1.1 and 0.7% for the single- and double-reinforced tests, respectively, occurred when using weaker gravel ($\varphi = 25^\circ$). When using stronger gravel that mobilized less confinement from the geocell, smaller strains occurred in the geocell (0.4 and 0.3% for single and double reinforced, respectively).

Implications of Numerical Analysis

Reasonable matching between the actual and simulated tests warrants further studies, such as behavior in a ballasted foundation for railways. Additionally, the effects of geocell stiffness or soil strength and stiffness can be observed, which could have significant economic implications in design. An in-depth parametric study on this geometry demonstrates that geocell is effective in improving the behavior of ballasted foundations for a large range of geocell stiffnesses, subgrade stiffnesses and ballast strengths (Leshchinsky and Ling 2013).

In the case of railroad construction, geocell would be installed no closer than 150 mm from the base of the tie to facilitate ballast construction and tamping. This clearance also assists in the maintenance process. Additionally, the upper portion of the ballasted foundation is exposed to high dynamic loads that could be damaging in proximity to the geocell. The minimum clearance between the geocell and the tie is reliant on maximum ballast grain size (typically below 63.5 mm in diameter according to industry standards). This constraint needs to be considered when modeling a ballasted railway foundation accurately, an aspect that further FE simulation could elucidate.

Actual field testing of such an application of geocell would also allow for observation of other relevant concerns, such as creep,

installation damage, higher amounts of loading cycles, ballast degradation, and foundation/subgrade effects. With actual field data, a FE analysis can again be validated and applied to a larger variety of applications with confidence. The work presented herein is a first step in such direction. Currently, field tests are in the final stages of planning, with implementation expected within the near future.

Conclusions

Experimental data obtained from a series of laboratory tests on gravel embankments with different configurations of geocell reinforcement suggested that application of its confining mechanism can yield higher stiffness, strength, and lower deformations compared with an unreinforced gravel embankment. A series of finite-element analysis simulation of these tests was performed in ABAQUS (Hibbitt, Karlsson and Sorensen Inc. 2007) to expand further studies on the effects of this material without the intensive resource requirements that model tests required. The general agreement between the experimental and simulated results indicates that there are significant benefits to using geocell confinement to increase the structural integrity of a gravel foundation. Some of the conclusions inferred from the results are as follows:

1. Geocell confinement minimized vertical settlement from occurring under both monotonic and cyclic loading conditions. This confining mechanism was also effective in preventing some of the lateral spreading that is to be expected as a result of this vertical loading;

2. The application of geocell inhibited continuous vertical displacement under cyclic loading;
3. Although the agreement between the actual and simulated lateral displacements was not perfect in either the monotonic or cyclic cases, the simulations still effectively demonstrated a trend of reduced deformation as a result of geocell confinement. In the cyclically loaded, reinforced tests, the vertical displacements did not match exactly, but again indicated the reduced deformations caused by use of geocell;
4. The lateral deformations that occurred in the experiments were difficult to simulate with FE analysis, especially with a simplified plasticity model using Drucker-Prager yield criterion. This could be because of the anisotropy and low confinement pressures encountered outside the geocell confinement (i.e., crest of embankment, outer profile of slope);
5. Observations of stresses and strains in the geocell in both the experiments and simulations generally agreed, especially in indicating the elastic behavior and low strains in the geocell. Additionally, the highest concentrations of stress and strain were found to be in the lower corners of the cell underlying the loading plate, likely caused by high tensile stresses in the reinforcement as a result of the significant vertical settlement under the loading plate and resultant bending behavior of the geocell/gravel composite. This suggests the importance of strong geocell seams, which could be critical under increased loading and/or more loading cycles; and
6. Parametric studies showed that implementation of geocell confinement demonstrates a significant benefit by distributing subgrade stresses more uniformly, as supported by previous field tests (Chrismer 1997). This is because of the mattress effect that the geocell composite displays when under loading (Zhou and Wen 2008). This reduction in maximum stress reduces settlement and increase bearing capacity. Additionally, when a competent foundation or weak gravel is present, the geocell prevents significant lateral spreading that would occur in the gravel because of the vertical loading and displacement at the crest of the model.

Further FE analysis studies on actual railroad ballasted foundation geometry in combination with a parametric analysis on varying material properties (i.e., strength or compressibility of subgrade, strength of geocell infill, stiffness of geocell) could have significant engineering and economic implications on this application of geocell confinement. Actual field testing and validation could yield useful data on relevant, yet difficult to predict, phenomena such as creep, higher magnitudes of loading cycles, and foundation effects.

Acknowledgments

The authors acknowledge information provided by Dr. Allan Zarembski of Zeta Tech; Steve Chrismer, Principal Engineer, Track Geometry and Roadbed Improvement of Amtrak; and PRS Mediterranean for partial support of this study. Additionally, the authors thank the reviewers for very useful, constructive, and thoughtful comments on the submission.

References

- ASTM. (2010). "Standard test method for tensile properties of plastics." *D638-10*, West Conshohocken, PA.
- Chrismer, S. (1997). "Test of Geoweb® to improve track stability over soft subgrade." *Rep. TD 97-045*, Technology Department, Association of American Railroads, Washington DC.
- Giroud, J. P., and Han, J. (2004). "Design method for geogrid-reinforced unpaved roads, Part I theoretical development." *J. Geotech. Geoenviron. Eng.*, 130(8), 776–786.
- Han, J., Leshchinsky, D., Parsons, R. L., Rosen, A., and Yuu, J. (2008). "Technical review of geocell-reinforced base courses over weak subgrade," Vol. 1.1, *Proc., 1st Pan-American Conf. and Exhibition*, Cancun, Mexico, 1022–1030.
- Hibbitt, Karlsson and Sorensen Inc. (2007). *ABAQUS user's manual, version 6.7*, Hibbitt, Karlsson and Sorensen Inc., Pawtucket, RI.
- Indraratna, B., Christie, D., Khabbaz, H., and Salim, W. (2006). "Geotechnical properties of ballast and the role of geosynthetics in rail track stabilisation." *Ground Improv.*, 10(3), 91–101.
- Indraratna, B., Ionescu, D., and Christie, D. (1998). "Shear behaviour of railway ballast based on large scale triaxial testing." *J. Geotech. Geoenviron. Eng.*, 124(5), 439–449.
- Indraratna, B., Nimbalkar, S., Christie, D., Rujikiatkamjorn, C., and Vinod, J. (2010). "Field assessment of the performance of a ballasted rail track with and without geosynthetics." *J. Geotech. Geoenviron. Eng.*, 136(7), 907–917.
- Indraratna, B., and Salim, W. (2002). "Modelling of particle breakage of coarse aggregates incorporating strength and dilatancy." *Proc., Institution of Civil Engineers, Geotechnical Engineering*, London, 243–252.
- Lackenby, J., Indraratna, B., McDowell, G., and Christie, D. (2007). "Effect of confining pressure on ballast degradation and deformation under cyclic triaxial loading." *Geotechnique*, 57(6), 527–536.
- Leshchinsky, B. (2011). "Enhancing ballast performance using geocell confinement." *Proc., Geo-Frontiers 2011*, Geo-Institute of ASCE, Dallas, TX, 4693–4072.
- Leshchinsky, B., and Ling, H. (2013). "Numerical modeling of behavior of railway ballasted structure with geocell confinement." *Geotext. Geomembranes*, 36, 33–43.
- Ling, H., Leshchinsky, D., Wang, J. P., Mohri, Y., and Rosen, A. (2009). "Seismic response of geocell retaining walls: Experimental studies." *J. Geotech. Geoenviron. Eng.*, 135(4), 515–524.
- Pokharel, S., et al. (2011). "Accelerated pavement testing of geocell-reinforced unpaved roads over weak subgrade." *10th Int. Conf. on Low-Volume Roads*, Journal of Transportation Research Board, Lake Buena Vista, FL, 67–75.
- Raymond, G. P. (2001). "Failure and reconstruction of a gantry crane ballasted track." *Can. Geotech. J.*, 38(3), 507–529.
- Selig, E., and Waters, J. (1994). *Track geotechnology and substructure management*, Thomas Telford Books, London.
- Webster, S. L., and Alford, S. J. (1977). "Investigation of construction concepts for pavement across soft ground." *Rep. S-77-1*, Soils and Pavements Laboratory, U.S. Army Engineer Waterways Experiment Station, Vicksburg, MS.
- Yang, X. (2010). "Numerical analyses of geocell-reinforced granular soils under static and repeated loads." Ph.D. thesis, Univ. of Kansas, Lawrence, KS.
- Zhou, H., and Wen, X. (2008). "Model studies on geogrid- or geocell-reinforced sand cushion on soft soil." *Geotextiles Geomembranes*, 26(3), 231–238.